

Pursuing Forecasts of the Behavior and Arrival of Coronal Mass Ejections through Modeling and Observations

Hebe Cremades^{1,2}

¹Universidad Tecnológica Nacional – Facultad Regional Mendoza, CEDS

²Consejo Nacional de Investigaciones Científicas y Técnicas (CONICET)

Rodríguez 243, 5500, Mendoza, Argentina

email: hebe.cremades@frm.utn.edu.ar

Abstract. Sophisticated instrumentation dedicated to studying and monitoring our Sun's activity has proliferated in the past few decades, together with the increasing demand of specialized space weather forecasts that address the needs of commercial and government systems. As a result, theoretical and empirical models and techniques of increasing complexity have been developed, aimed at forecasting the occurrence of solar disturbances, their evolution, and time of arrival to Earth. Here we will review groundbreaking and recent methods to predict the propagation and evolution of coronal mass ejections and their driven shocks. The methods rely on a wealth of data sets provided by ground- and space-based observatories, involving remote-sensing observations of the corona and the heliosphere, as well as detections of radio waves.

Keywords. Sun: coronal mass ejections (CMEs), solar-terrestrial relations, interplanetary medium

1. Introduction

The first hints of Sun-Earth connection were revealed in the mid-eighteenth century, as Olof Hiorter and Anders Celsius noticed perturbations in a geomagnetic needle in connection with aurorae. A century later, these magnetic disturbances were found to have the same frequency and phase as sunspots (Sabine 1852). Although several groundbreaking discoveries related with solar physics and solar-terrestrial relations followed in the years to come (*e.g.* Carrington 1859, Hale 1908, Fairfield & Cahill 1966), it was not until the beginning of the space age when coronal mass ejections (CMEs) were discovered. Their existence had been proposed to explain geomagnetic disturbances (see summary in Burlaga *et al.* 1991), so that CMEs were soon associated with magnetic interplanetary structures originating at the Sun (*e.g.* Schwenn 1983, Sheeley *et al.* 1985).

Ground- and space-based observatories dedicated to Heliophysics proliferated in the following years, enabling in-depth studies of the Sun's interior and atmosphere, as well as of its impact in the interplanetary medium, Earth, and other planets. Several aspects of CMEs came to light, regarding *e.g.* their source regions, kinematics, and morphology. In spite of significant progress on these matters, to date it has not been possible to foresee when and where on the Sun the next CME might take place. This limitation implies that forecasting must be based *sine qua non* with the occurrence of a CME, *i.e.* only once a CME has erupted, its arrival at Earth and degree of influence may be forecasted. The identification of Earth-directed CMEs has proven to be non-trivial, since it is mainly based on observations from white-light coronagraphs. Because of the Thomson scattering effect (*e.g.* Vourlidis & Howard 2006), Earth-directed CMEs may be at times undetected by coronagraphs located in the Sun-Earth line. This problem was addressed by Cremades *et al.* (2015a), who investigated the production of CMEs from an active region crossing

central meridian, and found twice as many CMEs traveling towards Earth when using coronagraphs located $\sim 90^\circ$ away from the Sun-Earth line, implying a significant number of missed alarms. In addition, a subset of events dubbed “stealth CMEs” (Robbrecht *et al.* 2009) may not leave perceptible imprints on low coronal images, complicating even more the identification of potentially geoeffective CMEs.

Once a CME is detected, a good assessment of the three-dimensional (3D) trajectory and size serves to determine *if* it will arrive at Earth, while knowledge on its propagation profile is crucial to ascertain *when* it will arrive. Furthermore, information on *how* the associated magnetic fields are configured is key to determine whether the Earth’s magnetosphere is to be disrupted and to what extent. In the next sections, I will briefly discuss tools and models that have been proposed to address these aspects.

2. Determining propagation direction and size

Soon after the discovery of CMEs, there was some speculation on whether CMEs could be best described as planar loops (Trottet & MacQueen 1980) or 3D structures (*e.g.* Howard *et al.* 1982, Crifo *et al.* 1983), with the latter being quickly accepted. Likewise, it did not take long to recognize that CMEs and their trajectories appear projected in the plane of the sky, thus hindering proper assessment of their 3D characteristics. This is particularly critical for events that propagate close to the Sun-Earth line, which are certainly the most threatening for the space weather at Earth. To overcome the problem for these events, particularly halo CMEs, cone models based on coronagraph observations were proposed before (*e.g.* Howard *et al.* 1982) and during the SOHO era beginning in the mid-1990s (SOHO: Solar and Heliospheric Observatory; Domingo *et al.* 1995). Some of these include Zhao *et al.* (2002), Michalek *et al.* (2003), Xie *et al.* (2004), Cremades & Bothmer (2005), Zhao (2008), and Na *et al.* (2013). The outcome of these models in terms of propagation direction and size is particularly useful to feed models of propagation and arrival time of CMEs and shocks (see Section 4).

Other ways of finding out the 3D propagation direction based on single-viewpoint observations rely on characteristics of the low-coronal environment at the time of eruption. This is the case of the methods proposed by Cremades *et al.* (2006) and Gopalswamy *et al.* (2009), which consider coronal holes as playing a key role in the deflection of CMEs from their source regions. Kay *et al.* (2013) developed a more sophisticated data-driven model of the coronal background that also takes into account CME properties to predict deflection for the first solar radii of propagation.

The launch of the STEREO mission in 2006 (Solar-Terrestrial Relations Observatory; Kaiser *et al.* 2008) enabled new ways of finding these CME attributes while minimizing uncertainties. The most widespread methods are either based on the tie-pointing/triangulation reconstruction (*e.g.* Temmer *et al.* 2009, Mierla *et al.* 2009, Srivastava *et al.* 2009, Liu *et al.* 2009, Liewer *et al.* 2011), polarization ratio (*e.g.* Moran *et al.* 2010, deKoning & Pizzo 2010) or forward modeling (*e.g.* Thernisien *et al.* 2009, Wood *et al.* 2010). The first method requires at least two viewpoints, and that the same parcel of coronal material can be discerned in stereoscopic images, which is not always straightforward. With the polarization ratio technique, however, observations from one viewpoint are enough, although multiple views are helpful to constrain the problem. Forward modeling approaches fit an *ad hoc* 3D density distribution to achieve visual agreement with data. Best results are obtained when applied to observations from three different viewpoints, while solutions are strongly undetermined for single vantage point observations. Unfortunately, these tools are often inappropriately used, because their limitations are overlooked and an untrained

eye may find various erroneous solutions that fit the same CME. For a comparison of these and other reconstruction techniques, see Mierla *et al.* (2009, 2010).

The interpretation of white-light images for size assessment must be taken with care, given that the outermost rim of a CME may represent the shock (Vourlidas *et al.* 2013), especially for the case of CMEs seen as halos. It should be noted that events that succeed to be seen as halo CMEs in past and present coronagraphs are indeed “special” (Lara *et al.* 2006), faster and wider than average (*e.g.* Shen *et al.* 2013). In fact, full limb halo CMEs –halo CMEs completely surrounding a coronagraph’s occulter but at the same time originating close to the solar limb– may be geoeffective (Gopalswamy *et al.* 2007, Cid *et al.* 2012), while a fairly bright and wide CME seen at the limb may not show up as a halo when changing vantage point by $\sim 90^\circ$ (Cremades *et al.* 2015a).

3. Determining flux rope orientation

A period of negative B_z component of the interplanetary magnetic field at 1 AU is well known for disrupting the Earth’s magnetic field. This can be provided by parts of the helical magnetic flux rope(s) embedded within interplanetary CMEs (ICMEs) or by the interplanetary magnetic field compressed ahead of the ICME. While the latter is more difficult to predict, requiring complex high-resolution dynamic 3D models of the ambient solar wind, potential geoeffectiveness of a white-light CME may be partially ascertained based on the knowledge of the configuration of its magnetic flux rope (see Vourlidas *et al.* 2013 for a discussion on the fraction of CMEs embedding flux ropes).

Bothmer & Schwenn (1998) recognized different magnetic field configuration patterns in Helios 1 and 2 in-situ data sets, in agreement with the helical magnetic flux rope picture. The magnetic configuration of filaments could be related to that of the so-called magnetic clouds detected in-situ, having four possible types, resulting from two possible directions of the field axis and two possible values of magnetic helicity or handedness. Although for the examined time interval they found that the axes of the flux ropes were generally close to the ecliptic plane, later studies identified other orientations (*e.g.* Mulligan *et al.* 2000, Huttunen *et al.* 2005, Lepping *et al.* 2006). The apparent relationship between the magnetic configuration of interplanetary flux ropes and that of their solar sources (*e.g.* Yurchyshyn 2008, Marubashi *et al.* 2015) has motivated a number of studies toward magnetic field prediction at 1 AU (Savani *et al.* 2015, 2017, Kay *et al.* 2017).

As stated above, CME deflection from their solar sources and rotation of their main axis are common effects in the first stages of eruption. While various approaches have been proposed to tackle the issue of deflection (see Section 2), only few studies address rotation (*e.g.* Vourlidas *et al.* 2011, Kay & Opher 2015, Kay *et al.* 2017). Instead of deducing CME rotation with respect to their source regions, at times it can be more convenient to determine flux rope orientation from white-light observations of CMEs, given that at heights of a few solar radii they have experienced most of these effects to eventually behave self-similarly. However, this is not an easy task, since orientations of the main axis of reconstructed CMEs have large uncertainties (Thernisien *et al.* 2009), which in turn may have large impact on the predictions of in-situ conditions through simulations of ICMEs (*e.g.* Savani *et al.* 2017, Kay *et al.* 2017). Stronger constraints on latitude, longitude, and tilt of the main axis of white-light CMEs can be achieved with a proper combination of vantage points and CME propagation direction. As shown by Cremades and Bothmer (2004), the projected morphology exhibited by CMEs depends on their propagation direction and orientation with respect to the vantage point (Figure 1a). If all remote-observing spacecraft as well as the CME trajectory approximately lie in the same plane, *i.e.* the ecliptic, to find the orientation of the CME’s main axis will involve

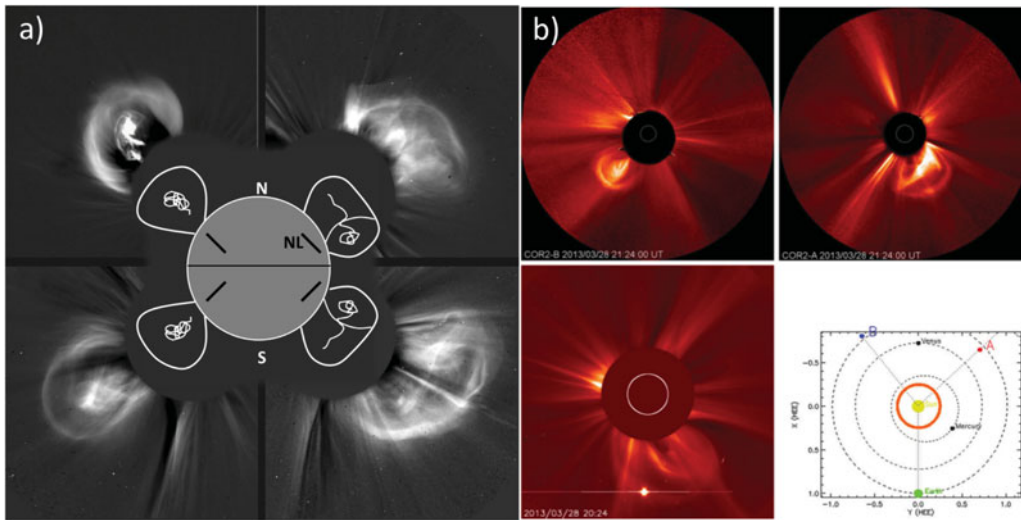


Figure 1. a) The 3D configuration scheme and four sample CMEs in agreement with it. The main symmetry axes of the CMEs to the East are oriented along the line of sight (axial view), while those to the West are aligned with the plane of the sky (lateral view). The black lines on the solar disk represent the neutral lines of the related source regions. Adapted from Cremades and Bothmer (2004). b) Axial (top-left) and lateral (top-right) views of the same CME, made possible from observations in quadrature respectively from STEREO B and A, and because of a nearly polar propagation and favorable orientation of the CME's main axis with respect to the vantage points. The bottom-left image is an intermediate view provided by SOHO. Bottom-right: location of the STEREO spacecraft relative to the Sun and Earth, with the CME traveling away from the ecliptic represented by the bold circle surrounding the Sun. From Cabello *et al.* (2016).

inherent uncertainties. Unfortunately, this is the case for most Earth-directed CMEs. To help reduce these uncertainties, a configuration in quadrature between vantage points and CME propagation direction is required. This problematic has been explained by Cabello *et al.* (2016), who presented the first simultaneous observation of both flux rope views for the same CME, which was possible for an event propagating nearly perpendicular to the ecliptic plane (Figure 1b). The upcoming Solar Orbiter mission will enable analogous observations for Earth-directed CMEs through observations from above the solar poles.

4. Determining time of arrival

Most of the forecasting models naturally focus on the forecasting of arrival times of CMEs and/or their associated shocks, provided that a CME with a propagation direction component toward Earth has been ejected. Inspired by the classification proposed by Zhao & Dryer (2014), forecasting models are here sorted into three classes: (i) empirical, data assimilative models, (ii) physics-based models, and (iii) magnetohydrodynamic (MHD) models. Empirical, data assimilative models rely on typically simple analytic expressions fed with parameters obtained from solar, coronal, or interplanetary detections. Examples of these are those by Gopalswamy *et al.* (2001, 2005), Wang *et al.* (2002), Srivastava & Venkatakrishnan (2004), Xie *et al.* (2006), and Michalek *et al.* (2008). Other approaches rely on the concept of radial and expansion speed of CMEs (Schwenn *et al.* 2005, Mäkelä *et al.* 2016). Prediction techniques may for instance also profit from interplanetary scintillation information (*e.g.* Jackson *et al.* 1998, Manoharan 2006), from heliospheric imaging (*e.g.* Sheeley *et al.* 2008, Rouillard *et al.* 2008, Davis *et al.* 2011, Colaninno *et al.* 2013, Möstl *et al.* 2014, Rollett *et al.* 2016), or from tomographic

considerations (*e.g.* Jackson *et al.* 2011). Low-frequency type II radio emissions can be useful to forecast CME shock arrival times, assuming that the emission takes place at the Earth-directed shock sector and that at those distances (farther than 30 solar radii) the shock propagates with nearly constant speed. Only one third of L1 shocks are associated to low-frequency type II events, however shock arrival times based on these emissions have errors of less than ± 6 h for 85% of the events (Cremades *et al.* 2015b).

Among the physics-based models the Shock Time of Arrival (STOA; Dryer & Smart 1984), the Interplanetary Shock Propagation Model (Smith & Dryer 1990), and the Hakamada-Akasofu-Fry (HAF) version 2 (Fry *et al.* 2003) stand out. Improvements to the STOA model have been proposed by Qin *et al.* (2009) and Liu & Qin (2012) on the basis of solar energetic particles and X-rays. The drag-based model assumes that the dominant force exerted on ICMEs is the magnetohydrodynamical equivalent of the aerodynamic drag (Vršnak *et al.* 2007, 2013). The aforementioned models have errors in time of arrival that range from ~ 6 to 12 h. Shi *et al.* (2015) and Hess & Zhang (2015) have proposed a combination of stereoscopic measurements with the drag-based model, to achieve average errors of 8.6 h for 16 events, and under 3.5 h for seven events respectively. The Shock Propagation Model version 3 by Zhao & Feng (2015) was applied to over 200 Earth-directed events to yield an average absolute error of ~ 9 h.

Several of the most renowned MHD models are routinely used for space weather prediction purposes. Enlil may be constrained by the Wang-Sheeley-Argge (WSA) method and/or a cone model (Odstrcil *et al.* 2004, 2005, Xie *et al.* 2013). CORHEL uses a coronal model (Magnetohydrodynamics outside A Sphere–MAS or WSA) combined with a heliospheric model (MAS or Enlil) (Linker *et al.* 2009). The Alfvén-Wave driven solar wind Model (AWSOM), part of the Space Weather Modeling Framework, is based on the BATS-R-US code (Tóth *et al.* 2005, 2012, Van der Holst *et al.* 2014) and can be used in combination with the Eruptive Event Generator – Gibson and Low (Jin *et al.* 2017). The HAF version 3 combined with the 3D MHD model by Wu *et al.* (2007, 2011), and the Solar-InterPlanetary Conservation Element/Solution Element MHD model by Feng *et al.* (2007, 2010) are other prediction models of widespread use.

The inherent uncertainties of input parameters, the limited knowledge on how kinematics and morphology behave for different events, and the difficulties in determining the real solar wind conditions in 3D space and time are the main factors that affect the performance of existing models (Zhao & Dryer 2014). This includes interactions between transients and with other structures (*e.g.* Dasso *et al.* 2009, Liu *et al.* 2012, Lugaz *et al.* 2013, Temmer *et al.* 2014). According to Burlaga (2002), two out of three ICMEs are complex events, which implies that realistic simulations require a high level of complexity.

5. Final remarks

In the past three decades, diversity and progress of Heliophysics-dedicated space missions and ground-based observatories have enabled enormous advancement and increasing complexity of techniques and models aimed at forecasting CME behavior and arrival. However, the various techniques and models have different caveats, pros and cons, *e.g.* with respect to simplicity, running time, lead time, data assimilation, and number of events on which they have been validated. At the present time, the maximum benefit can only be achieved by recognizing which methods or models perform best under different circumstances, not only to avoid false and missed alarms, but also to obtain good proxies of arrival time. Furthermore, coronagraphs and EUV imagers, particularly those offset from the Sun-Earth line, are compelling to identify Earth-directed events and forecast their time of arrival.

Acknowledgements

HC is member of the Carrera del Investigador Científico (CONICET). She thanks the invitation and financial aid provided by the SOC and LOC of this IAU Symposium. She appreciates support from Argentine grants PICT 2012-973 (ANPCyT), PIP 2012-01-403 (CONICET) and UTI4035TC (UTN). The author is grateful to Fernando López for help with this manuscript. This proceeding is dedicated to the memory of Rainer Schwenn.

References

- Bothmer, V. & Schwenn, R. 1998, *Annales Geophysicae*, 16, 1
- Burlaga, L. F. E. 1991, *Physics and Chemistry in Space*, 21, 1
- Burlaga, L. F., Plunkett, S. P. & St. Cyr, O. C. 2002, *J. Geophys. Res.*, 107, 1266
- Cabello, I., Cremades, H., Balmaceda, L. & Dohmen, I. 2016, *Solar Phys.*, 291, 1799
- Carrington, R. C. 1859, *Mon. Not. R. Astron. Soc.*, 20, 13
- Cid, C., Cremades, H., Aran, A., Mandrini, C., *et al.* 2012, *J. Geophys. Res.*, 117, A11102
- Colaninno, R. C., Vourlidas, A. & Wu, C. C. 2013, *J. Geophys. Res.*, 118, 6866
- Cremades, H. & Bothmer, V. 2004, *A&A*, 422, 307
- Cremades, H. & Bothmer, V. 2005, *IAU Symp. No 226, Dere, K., Wang, J. & Yan, Y. (eds.)*
- Cremades, H., Bothmer, V. & Tripathi, D. 2006, *Adv. Space Res.*, 38, 461
- Cremades, H., Mandrini, C. H., Schmieder, B. & Crescitelli, A. M. 2015a, *Solar Phys.*, 290, 1671
- Cremades, H., Iglesias, F. A., St. Cyr, O. C., Xie, H., *et al.* 2015b, *Solar Phys.*, 290, 2455
- Crifo, F., Picat, J. P. & Cailloux, M. 1983, *Solar Phys.*, 83, 143
- Dasso, S., Mandrini, C., Schmieder, B., Cremades, H., *et al.* 2009, *J. Geophys. Res.*, 114, A02109
- Davis, C. J., de Koning, C. A., Davies, J. A., Biesecker, D., *et al.* 2011, *Space Weather*, 9, S01005
- Dryer, M. & Smart, D. F. 1984, *Adv. Space Res.*, 4, 291
- de Koning, C. A. & Pizzo, V. J. 2010, *AGU Fall Meeting Abstracts*
- Domingo, V., Fleck, B. & Poland, A. I. 1995, *Solar Phys.*, 162, 1
- Fairfield, D. H. & Cahill, Jr., L. J. 1966, *J. Geophys. Res.*, 71, 155
- Feng, X., Zhou, Y. & Wu, S. T. 2007, *ApJ*, 655, 1110
- Feng, X., Yang, L., Xiang, C., Wu, S. T., *et al.* 2010, *ApJ*, 723, 300
- Fry, C. D., Dryer, M., Smith, Z., Sun, W., *et al.* 2003, *J. Geophys. Res.*, 108, 1070
- Gopalswamy, N., Lara, A., Yashiro, S., Kaiser, M. L., *et al.* 2001, *J. Geophys. Res.*, 106, 29207
- Gopalswamy, N., Lara, A., Manoharan, P. K. & Howard, R. A. 2005, *Adv. Space Res.*, 36, 2289
- Gopalswamy, N., Yashiro, S. & Akiyama, S. 2007, *J. Geophys. Res.*, 112, A06112
- Gopalswamy, N., Mäkelä, P., Xie, H., Akiyama, S., *et al.* 2009, *J. Geophys. Res.*, 114, A00A22
- Hale, G. E. 1908, *ApJ*, 28, 315
- Hess, P. & Zhang, J. 2015, *ApJ*, 812, 144
- Howard, R. A., Michels, D. J., Sheeley, N. R. & Koomen, M. J. 1982, *ApJ (L)*, 263, L101
- Huttunen, K. E. J., Schwenn, R., Bothmer, V. & Koskinen, H. 2005, *Ann. Geophys.*, 23, 625
- Jackson, B. V., Hick, P. L., Kojima, M. & Yokobe, A. 1998, *J. Geophys. Res.*, 103, 12049
- Jackson, B. V., Hamilton, M. S., Hick, P. P., *et al.* 2011, *J. Atmos. Sol-Terr. Phys.*, 73, 1317
- Jin, M., Manchester, W. B., van der Holst, B., Sokolov, I., *et al.* 2017, *ApJ*, 834, 173
- Kaiser, M. L., Kucera, T. A., Davila, J. M., St. Cyr, O. C., *et al.* 2008, *Space Sci. Rev.*, 136, 5
- Kay, C. & Opher, M. 2015, *ApJ (L)*, 811, L36
- Kay, C., Opher, M. & Evans, R. M. 2013, *ApJ*, 775, 5
- Kay, C., Gopalswamy, N., Reinard, A. & Opher, M. 2017, *ApJ*, 835, 117
- Lara, A., Gopalswamy, N., Xie, H., Mendoza-Torres, E., *et al.* 2006, *J. Geophys. Res.*, 111, 6107
- Lepping, R. P., Berdichevsky, D. B., Wu, C.-C., Szabo, A., *et al.* 2006, *Ann. Geophys.*, 24, 215
- Liewer, P. C., Hall, J. R., Howard, R. A., *et al.* 2011, *J. Atmos. Sol-Terr. Phys.*, 73, 1173
- Linker, J. A., Riley, P., Mikic, Z., Lionello, R., *et al.* 2009, *AGU Fall Meeting Abstracts*
- Liu, H.-L. & Qin, G. 2012, *J. Geophys. Res.*, 117, A04108
- Liu, Y., Luhmann, J. G., Lin, R. P., Bale, S. D., *et al.* 2009, *ApJ (L)*, 698, L51
- Liu, Y. D., Luhmann, J. G., Möstl, C., Martinez-Oliveros, J. C., *et al.* 2012, *ApJ (L)*, 746, L15

- Lugaz, N., Farrugia, C. J., Manchester, IV, W. B. & Schwadron, N. 2013, *ApJ*, 778, 20
- Mäkelä, P., Gopalswamy, N. & Yashiro, S. 2016, *Space Weather*, 14, 368
- Manoharan, P. K. 2006, *Solar Phys.*, 235, 345
- Marubashi, K., Akiyama, S., Yashiro, S., Gopalswamy, N., *et al.* 2015, *Solar Phys.*, 290, 1371
- Michalek, G., Gopalswamy, N. & Yashiro, S. 2003, *ApJ*, 584, 472
- Michalek, G., Gopalswamy, N. & Yashiro, S. 2008, *Solar Phys.*, 248, 113
- Mierla, M., Inhester, B., Marqué, C., Rodriguez, L., *et al.* 2009, *Solar Phys.*, 259, 123
- Mierla, M., Inhester, B., Antunes, A., Boursier, Y., *et al.* 2010, *Ann. Geophys.*, 28, 203
- Moran, T. G., Davila, J. M. & Thompson, W. T. 2010, *ApJ*, 712, 453
- Möstl, C., Amla, K., Hall, J. R., Liewer, P. C., *et al.* 2014, *ApJ*, 787, 119
- Mulligan, T., Russell, C. T. & Luhmann, J. G. 2000, *Adv. Space Res.*, 26, 801
- Na, H., Moon, Y.-J., Jang, S., Lee, K.-S., *et al.* 2013, *Solar Phys.*, 288, 313
- Odstrcil, D., Riley, P. & Zhao, X. P. 2004, *J. Geophys. Res.*, 109, A02116
- Odstrcil, D., Pizzo, V. J. & Arge, C. N. 2005, *J. Geophys. Res.*, 110, A02106
- Qin, G., Zhang, M. & Rassoul, H. K. 2009, *J. Geophys. Res.*, 114, A09104
- Robbrecht, E., Patsourakos, S. & Vourlidas, A. 2009, *ApJ*, 701, 283
- Rollett, T., Möstl, C., Isavnin, A., Davies, J. A., *et al.* 2016, *ApJ*, 824, 131
- Rouillard, A. P., Davies, J. A., Forsyth, R. J., Rees, A., *et al.* 2008, *Geophys. Res. (L)*, 35, L10110
- Sabine, E. 1852, *Phil. Trans. R. Soc. Lond.*, 142, 103
- Savani, N. P., Vourlidas, A., Szabo, A., Mays, M. L., *et al.* 2015, *Space Weather*, 13, 374
- Savani, N. P., Vourlidas, A., Richardson, I. G., Szabo, A., *et al.* 2017, *Space Weather*, 15, 441
- Schwenn, R. 1983, *Space Sci. Rev.*, 34, 85
- Schwenn, R., dal Lago, A., Huttunen, E. & Gonzalez, W. D. 2005, *Ann. Geophys.*, 23, 1033
- Shen, C., Wang, Y., Pan, Z., Zhang, M., *et al.* 2013, *J. Geophys. Res.*, 118, 6858
- Sheeley, Jr., N., Howard, R. A., Michels, D., Koomen, M., *et al.* 1985, *J. Geophys. Res.*, 90, 163
- Sheeley, Jr., N. R., Herbst, A. D., Palatchi, C. A., Wang, Y.-M., *et al.* 2008, *ApJ*, 675, 853
- Shi, T., Wang, Y., Wan, L., Cheng, X., *et al.* 2015, *ApJ*, 806, 271
- Smith, Z. & Dryer, M. 1990, *Solar Phys.*, 129, 387
- Srivastava, N. & Venkatakrishnan, P. 2004, *J. Geophys. Res.*, 109, A10103
- Srivastava, N., Inhester, B., Mierla, M. & Podlipnik, B. 2009, *Solar Phys.*, 259, 213
- Temmer, M., Preiss, S. & Veronig, A. M. 2009, *Solar Phys.*, 256, 183
- Temmer, M., Veronig, A. M., Peinhart, V. & Vršnak, B. 2014, *ApJ*, 785, 85
- Thernisien, A., Vourlidas, A. & Howard, R. A. 2009, *Solar Phys.*, 256, 111
- Tóth, G., Sokolov, I. V., Gombosi, T., Chesney, D., *et al.* 2005, *J. Geophys. Res.*, 110, A12226
- Tóth, G., van der Holst, B., Sokolov, I., De Zeeuw, D., *et al.* 2012, *J. Comput. Phys.*, 231, 870
- Trottet, G. & MacQueen, R. M. 1980, *Solar Phys.*, 68, 177
- van der Holst, B., Sokolov, I. V., Meng, X., Jin, M., *et al.* 2014, *ApJ*, 782, 81
- Vourlidas, A. & Howard, R. A. 2006, *ApJ*, 642, 1216
- Vourlidas, A., Colaninno, R., Nieves-Chinchilla, T. & Stenborg, G. 2011, *ApJ (L)*, 733, L23
- Vourlidas, A., Lynch, B. J., Howard, R. A. & Li, Y. 2013, *Solar Phys.*, 284, 179
- Vršnak, B. & Žic, T. 2007, *A&A*, 472, 937
- Vršnak, B., Žic, T., Vrbanc, D., Temmer, M., *et al.* 2013, *Solar Phys.*, 285, 295
- Wang, Y. M., Ye, P. Z., Wang, S., Zhou, G. P., *et al.* 2002, *J. Geophys. Res.*, 107, 1340
- Wood, B. E., Howard, R. A. & Socker, D. G. 2010, *ApJ*, 715, 1524
- Wu, C.-C., Fry, C. D., Wu, S. T., Dryer, M., *et al.* 2007, *J. Geophys. Res.*, 112, A09104
- Wu, C.-C., Dryer, M., Wu, S. T., Wood, B. E., *et al.* 2011, *J. Geophys. Res.*, 116, A12103
- Xie, H., Ofman, L. & Lawrence, G. 2004, *J. Geophys. Res.*, 109, 3109
- Xie, H., Gopalswamy, N., Ofman, L., St. Cyr, O. C., *et al.* 2006, *Space Weather*, 4, 10002
- Xie, H., St. Cyr, O. C., Gopalswamy, N., Odstrcil, D., *et al.* 2013, *J. Geophys. Res.*, 118, 4711
- Yurchyshyn, V. 2008, *ApJ (L)*, 675, L49
- Zhao, X. P. 2008, *J. Geophys. Res.*, 113, 2101
- Zhao, X. P., Plunkett, S. P. & Liu, W. 2002, *J. Geophys. Res.*, 107, 1223
- Zhao, X. & Dryer, M. 2014, *Space Weather*, 12, 448
- Zhao, X. H. & Feng, X. S. 2015, *ApJ*, 809, 44